ELECTRONIC SUPPLEMENTARY INFORMATION

Products and Mechanism of Thermal Decomposition of Chlorpyrifos under Inert and Oxidative Conditions

Nathan H. Weber[a], Sebastian P. Stockenhuber[a], Emad Benhelal[a], Charles C. Grimison[b], John A. Lucas[a], John C. Mackie[a], Michael Stockenhuber[a] and Eric M. Kennedy[a]**

[a] Discipline of Chemical Engineering, School of Engineering,
University of Newcastle, Callaghan, NSW, 2308, AUSTRALIA.

[b] Ventia, Rhodes Corporate Park, 1 Homebush Drive, Rhodes, NSW 2138, AUSTRALIA

S1. EXPERIMENTAL APPARATUS AND METHODOLOGY

A flow reactor has been designed to study the thermal decomposition of CPF. The experimental design was predicated on the production of gaseous CPF from the solid material (Hangzhou Yuhao Chemical Technology Co, China, 98.4%) and the flow of its vapour through a three-zone furnace (Figure S1), with the same procedure adopted for TCpyol (Bide Pharmatech, China, 98.65%). The three-zone furnace was configured to allow the vaporizer zone to operate at 104 °C and the reactor zone, with an operating range between 500 to 850 °C. An alumina tube (6 mm od) fitted with Swagelok® connected Teflon tubing was placed inside the furnace forming the main reaction chamber shown in Figure S2. A Mass Flow controller (MFC) allowed controlled flow of either N_2 or air through each zone in a high purity alumina reactor tube

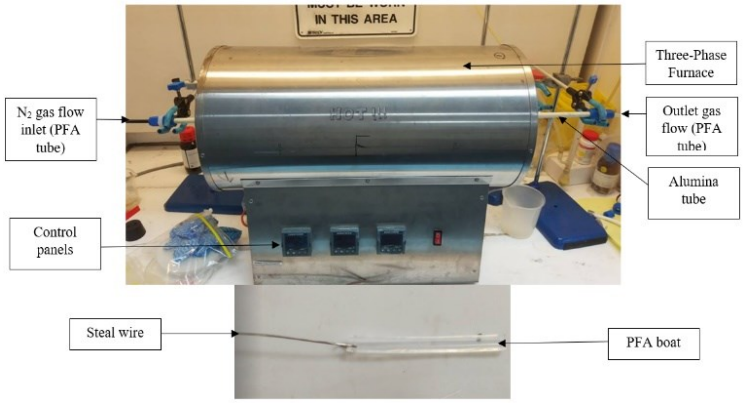

Figure S1. The main features of the apparatus three-zone furnace and boat.

To charge the CPF inside the furnace, a novel method was designed in which a fully charged container (boat) of 100 mg of solid CPF placed inside the vaporiser zone. The vaporised CPF flowed in the reactor at a residence time between 10 and 90 s. The container was made from PFA, which allowed durability and gave the capability for a wire to be placed in the container, reducing the chance for mass to be lost when removing unreacted CPF from the furnace.

Slight variations were completed for the TCP experiments where the vaporiser was increased to 300 °C and alumina was used as the container to carry the solid TCP into the vaporiser.

The primary analysis tool was an FT-IR (Perkin Elmer Spectrum 100, 11 cm path length Teflon gas cell fitted with 25 x 5 mm KBr windows) which detected gaseous products. Further, gas samples were captured for analysis through Shimadzu GCMS-QP5000 (Plot-Q column 30 m x 0.32 mm), and all exiting tubing was rinsed with toluene allowing soluble solid/liquid products to be analysed by the Agilent GC 6890 MS 5973N (HP-5MS column 30 m x 0.25 mm). A full schematic of the three-zone furnace is illustrated in Figure S2.

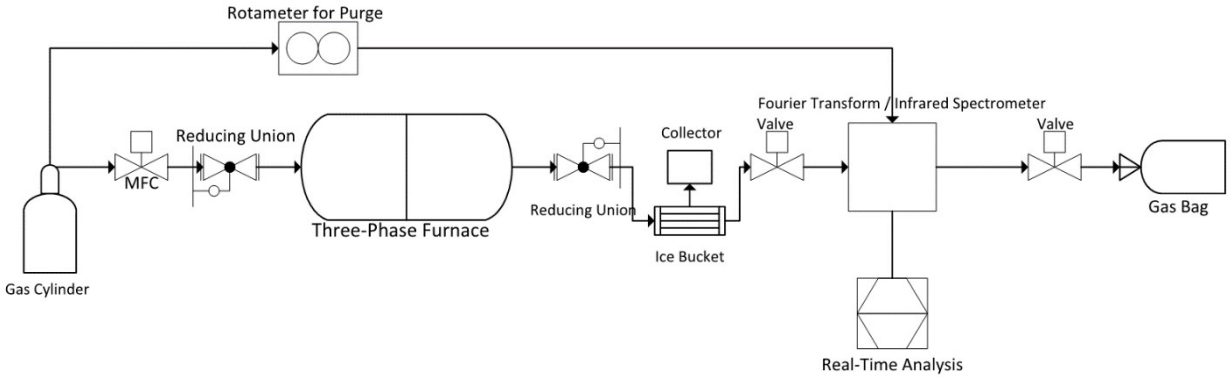

Figure S2. Diagram of the system used for the experimental reactions.

S2. GC/MS methodology and report

Shimadzu- GC17a MS-QP5000

The Shimadzu GCMS-QP5000 is designed for analysis of vapour phase samples. It includes the GC-17A which is the Gas Chromatograph section, an oven with a Plot-Q column 30 m x 0.32 mm diameter AT-Q with a Heliflex capillary, a QP5000 MS and sample injector.

The settings for the gas sample injection used were: Oven Temp: 30 °C (6 min); 10 °C/min to 220 °C (17 min hold); Injector temperature: 170 °C Scan range of 10 M/Z to 600 M/Z; A carrier gas of Helium (3.3 mL/min).All gas samples were analysed through the Shimadzu GCMS-QP5000 (Plot-Q column 30 m x 0.32 mm). For the temperatures above 650 °C under pyrolysis conditions (inert N_2) the decomposition of CPF gas products are seen in Table S1.

Table S1. GC/MS table report for the gas phase products of the pyrolysis of CPF at temperatures above 650 °C

Peak number	**RT (mins)**	**Name of compound**	**Molecular formula**	**MW (g/mol)**
1	2.342	Nitrogen, CO and other light gases	N_2	28.01
2	5.048	Ethylene	C_2H_4	28.05
3	9.000	Acetylene	C_2H_2	26.04
4	11.64	Chloroethylene	C_2H_3Cl	62.50
5	15.4	Hydrogen Cyanide	HCN	27.03
6	17.9	Carbon Monoxide	CO	28.01
6	19.3	1-Butyne	C_4H_6	54.09
7	19.4	1,3-Butadiene	C_4H_6	54.09
8	20.9	Acetonitrile	C_2H_3N	41.05
9	21.1	2-Propenenitrile	C_3H_3N	53.06
10	22.1	Carbon disulfide	CS_2	76.14
11	22.9	Cyanogen	C_2N_2	52.03

Agilent- GC 6890 MS 5973N

The Agilent 6890 is made up of the 6890 Gas Chromatography, an Agilent 5973 MS, a HP-5MS column with the dimensions 30 m x 0.25 mm diameter and a 0.25 μm film thickness.

The Agilent GC uses liquid samples. The settings for the liquid sample injection were: Oven Temp: 50 °C (2 min); 10 °C/min to 280 °C (5 min hold); Injector temperature: 260 °C; A carrier gas of Helium (1.5 mL/min).

CPF and TCpyol was identified using authentic standards. All unknown products were compared and found through the NIST database. All high resolution mass spectra were compared to the databased allowing the Agilent software ChemWindow to make a similarity match of 99% for all unknowns.

S3. INTERSYSTEM CROSSING

(a) CASSF calculations

The cyclic thiirane molecule, c-C_2H_4S, postulated as an important intermediate in the production of carbon disulfide from chlorpyrifos, can undergo ring-opening to the biradical, •CH_2CH_2S•. The biradical can exist in both singlet and triplet forms, however, since thiirane is a closed-shell singlet molecule, spin conservation would require initial formation of the singlet, ^{1}•CH_2CH_2S•. As the triplet form, ^{3}•CH_2CH_2S•, is a "pure" biradical, it can be treated by single configurational quantum mechanical methods such as MP2 or DFT and energies can be obtained by accurate methods such as Gn. However, the singlet has partial ionic form along with biradical nature and cannot be treated accurately by single configurational methods. As described in our paper, DFT and MP2 methods do not find the singlet form to be a stable minimum on the C_2H_4S potential energy surface (PES). These methods lead to triplet spin instability in the singlet wave function. Ultimately, the appropriate treatment is a multiconfiguational approach such as CASSCF (Complete Active Space SCF) although this does not generally lead to accurate energies and other thermodynamic properties.

We have therefore made a CASSCF(6,6) (6 electrons in 6 orbitals) study of the singlet and triplet biradicals. Starting with the triplet structure which had been optimised at M06-2X/6-31+G(d,p), orbitals chosen were the two singly occupied orbitals, one each on the S atom and the terminal methylene C atom, together with the two highest doubly occupied orbitals and two virtual orbitals. Similar orbitals were chosen for the singlet studies. Optimisations of singlet and triplet biradicals were carried out using three basis sets. All produced stable structures for both singlet and triplet biradicals with the triplet lower lying. Table S2 compares electronic energies (E_{elec}) for the three CAS computations along with the DFT results obtained at M06-2X/GTLarge//M06-2X/6-31+G(d,p). Also shown are the singlet-triplet interval (S-T). Also shown are E_{elec} for thiirane.

Table S2: Electronic energies/hartree for the •CH_2CH_2S• biradicals calculated by CASSCF(6,6) and DFT

	CASSCF(6,6)			DFT
	6-31G(d,p)	cc-pVDZ	cc-pVTZ	GTLarge
Singlet (S)	-475.53660147	-475.55542274	-475.59167442	-476.67896131[a]
Triplet (T)	-475.54358299	-475.56291825	-475.59899501	-476.68182172
S-T /kJ mol^{-1}	-18.3	-19.7	-19.2	-7.5
c-C_2H_4S	-475.619243695	-475.637013755	-475.676374186	-476.77205120

[a] Not a minimum on PES.

Geometrical parameters of the biradicals are listed in Table S3 for the DFT and CAS optimisations.

Table S3: Optimised geometry of biradicals (in Å and °)

	DFT		CASSCF(6,6)/6-31G(d,p)	
Geometry	singlet	triplet	singlet	triplet
S-C2	1.799	1.844	1.851	1.885
C1-C2	1.484	1.473	1.494	1.480
C1-H3	1.084	1.083	1.096	1.074
C1-H4	1.082	1.083	1.073	1.074
C2-H5	1.102	1.096	1.089	1.108
C2-H6	1.102	1.096	1.086	1.108
SĈ1C2	117.5	113.4	116.2	114.2
H3Ĉ1C2	119.5	120.1	118.4	119.5
H4Ĉ1C2	121.1	120.1	120.7	119.5

(b) Landau-Zener crossing probability

The SCC angles in the reactant, c-C_2H_4S, are 65.85°. As ring opening takes place, the SCC bond angle will increase progressively. By increasing this angle in increments of 5°, we can plot out the diabatic singlet state potential energy curve. We have used DFT optimisations to plot out a relaxed scan as a function of increasing SĈC ensuring that we have removed triplet-state instabilities from the singlet wavefunction. Likewise, starting with the optimised triplet biradical, we can decrease the SC1C2 angle progressively by 5° and plot out the diabatic triplet potential energy curve. As the triplet state is lower lying, the two diabatic curves will cross. The two curves are shown in Figure S3.

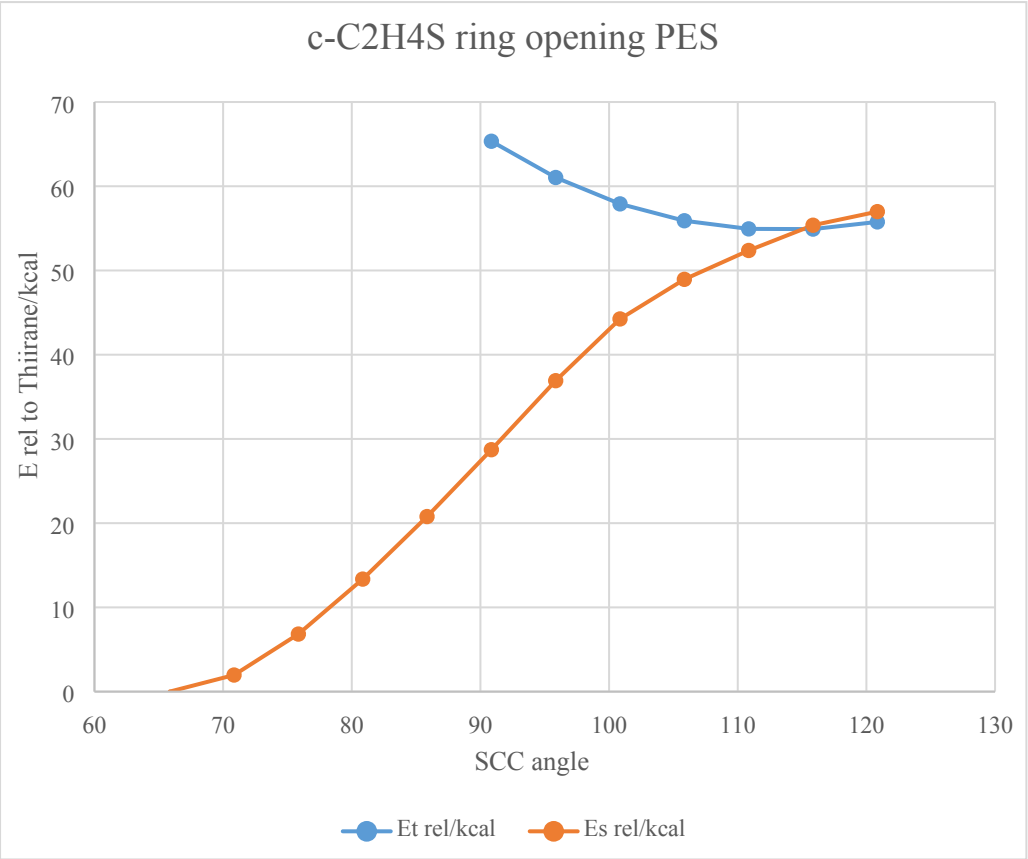

Figure S3: Diabatic crossing potential energy curves. E_t – triplet, Es – singlet. Energies are relative to that of thiirane.

From Figure S3 we see that the singlet curve crosses the triplet at an SCC angle of approximately 115°, quite close to the minimum in the triplet curve.

We wish to determine the probability of intersystem crossing in the vicinity of the crossing point. The Landau-Zener crossing formula can give a semi-quantitative estimate of this probability. The probability of a transition between two *adiabatic* surfaces is

$$P_{LZ} = \exp\left(-4\pi^2 H^2_{SO}/hv|\Delta F|\right)$$

where H_{SO} is the spin-orbit splitting, v is the mean one-dimensional velocity, $|\Delta F|$ is the difference in potential energy gradients of the two diabatic surfaces in the vicinity of the crossing point, and h is Planck's constant.

To determine the gradient difference, $|\Delta F| = |F_T - F_S|$, we need to convert angle into distance to determine $|\Delta F| = 4.63 \times 10^{-10}$ J m^{-1}. For the crossing velocity, v, we use the mean velocity in one dimension:

$$v = (2k_B T/\pi\mu)^{1/2}$$

where k_B is Boltzmann's constant, T is temperature, evaluated at 1000 K and μ is the reduced mass of the atoms undergoing the crossing. This last quantity is obtained from the reduced mass associated the frequency of the SĈC bend in the biradicals. Here $\mu = 4.95\times10^{-27}$ kg.

The spin-orbit coupling was obtained at CASSCF(6,6)/6-31G(d,p) as 188 cm^{-1}. This led to a value for P_{LZ} = 0.261. Finally, the probability of singlet-triplet intersystem crossing is estimated by

$$1 - P_{LZ} = 0.739$$

We can use this estimate as a multiplying factor in the evaluation for the canonical rate constant for the reaction

$$c\text{-}C_2H_4S \rightarrow [^1\bullet CH_2CH_2S\bullet\,] \rightarrow {}^3\bullet CH_2CH_2S\bullet \qquad \text{(SR1)}$$

The rate constant k_{RS1} is then expressed as

$$k_{RS1} = (1-P_{LZ})\,(k_B T/h)\,\exp(\Delta S_{cr}/R)\,\exp(-\Delta E_{cr}/RT)$$

where ΔS_{cr} and ΔE_{cr} are the differences in entropy and energy between the crossing point and the reactant and we can approximate these values with the differences between the singlet values and those of the reactant.

S4. ATOMIC COORDINATES

Please note: Only coordinates of substances not previously listed in our earlier publication (Kennedy, E. M.; Mackie, J. C., Mechanism of the Thermal Decomposition of Chlorpyrifos and Formation of the Dioxin Analog, 2,3,7,8-Tetrachloro-1,4-dioxino-dipyridine (TCDDpy). *Environ Sci Technol* **2018,** *52* (13), 7327-7333.) are given here.

The majority of substances studied in the present work have been optimised at the M06-2X/6-31+G(d,p) level of theory.

c-C_2H_4S

Centre Number	Atomic Number	Atomic Type	Coordinates (Angstroms) X	Y	Z
1	6	0	-1.939802	0.764508	-0.330350
2	6	0	-1.614288	0.239201	1.017638
3	1	0	-2.984093	0.810058	-0.621515
4	1	0	-1.313432	1.552051	-0.736239
5	1	0	-0.763780	0.664809	1.539917
6	1	0	-2.434673	-0.076644	1.653717
7	16	0	-1.204427	-0.892025	-0.337922

^{3}•CH_2CH_2S•

Centre Number	Atomic Number	Atomic Type	Coordinates (Angstroms) X	Y	Z
1	6	0	1.645072	-0.338063	0.000000
2	6	0	0.532735	0.627694	0.000000
3	1	0	1.969643	-0.791644	0.928049
4	1	0	1.969643	-0.791644	-0.928049
5	1	0	0.538358	1.280108	0.880102
6	1	0	0.538358	1.280108	-0.880102
7	16	0	-1.130218	-0.169731	0.000000

^{1}•CH_2CH_2S•

Centre Number	Atomic Number	Atomic Type	Coordinates (Angstroms) X	Y	Z
1	6	0	1.523121	0.415889	0.000000
2	6	0	0.405584	-0.461402	0.000000
3	1	0	2.527744	0.000510	0.000000
4	1	0	1.413658	1.498219	0.000000
5	1	0	0.646522	-1.189760	-0.818490
6	1	0	0.646522	-1.189760	0.818490
7	16	0	-1.292155	-0.089223	0.000000

CH_3CHS triplet

Centre Number	Atomic Number	Atomic Type	Coordinates (Angstroms) X	Y	Z
1	6	0	1.523121	0.415889	0.000000
2	6	0	0.405584	-0.461402	0.000000
3	1	0	2.527744	0.000510	0.000000
4	1	0	1.413658	1.498219	0.000000
5	1	0	0.646522	-1.189760	-0.818490
6	1	0	0.646522	-1.189760	0.818490
7	16	0	-1.292155	-0.089223	0.000000

CH2CHSH triplet

Centre Number	Atomic Number	Atomic Type	Coordinates (Angstroms) X	Y	Z
1	6	0	-1.722842	-0.226300	0.002905
2	6	0	-0.518473	0.584288	-0.026301
3	1	0	-2.217184	-0.531197	-0.915354
4	1	0	-2.134917	-0.598636	0.937913
5	1	0	1.799580	0.879610	-0.021520
6	1	0	-0.532958	1.659586	0.117588
7	16	0	1.033336	-0.222331	0.001359

HCS

Centre Number	Atomic Number	Atomic Type	Coordinates (Angstroms) X	Y	Z
1	6	0	1.402257	0.636636	0.403211
2	1	0	1.666159	1.671731	0.631733
3	16	0	0.048013	-0.138657	0.440056

HCSS

Centre Number	Atomic Number	Atomic Type	Coordinates (Angstroms) X	Y	Z
1	6	0	0.398874	0.609003	0.053480
2	1	0	0.480464	1.692110	0.141310
3	16	0	-1.042128	-0.208133	-0.032679
4	16	0	1.701062	-0.416631	-0.009791

SH

Centre Number	Atomic Number	Atomic Type	Coordinates (Angstroms) X	Y	Z
1	16	0	0.000000	-0.000000	0.079108

2	1	0	-0.000000	0.000000	-1.265722

CS

Centre Number	Atomic Number	Atomic Type	Coordinates (Angstroms) X	Y	Z
1	6	0	0.000000	0.000000	-1.116907
2	16	0	0.000000	0.000000	0.415143

H_2S

Centre Number	Atomic Number	Atomic Type	Coordinates (Angstroms) X	Y	Z
1	16	0	-0.507731	1.447157	0.000000
2	1	0	0.812881	1.646760	0.000000
3	1	0	-0.760405	2.758650	0.000000

CS_2

Centre Number	Atomic Number	Atomic Type	Coordinates (Angstroms) X	Y	Z
1	6	0	0.000000	0.000000	0.000000
2	16	0	0.000000	0.000000	1.554462
3	16	0	0.000000	0.000000	-1.554462

c-C_2H_3

Centre Number	Atomic Number	Atomic Type	Coordinates (Angstroms) X	Y	Z
1	6	0	-0.630437	0.849485	-0.146101
2	6	0	-0.960386	-0.560748	0.018285
3	1	0	-0.915158	1.711803	0.442916
4	1	0	-1.346262	-0.929773	0.967039
5	1	0	-1.268076	-1.127746	-0.856223
6	16	0	0.817152	-0.086669	0.013323

CH_2CHS

Centre Number	Atomic Number	Atomic Type	Coordinates (Angstroms) X	Y	Z
1	6	0	-0.500731	0.489311	0.000122
2	6	0	-1.551722	-0.333107	-0.000013

3	1	0	-0.639738	1.571022	-0.000097
4	1	0	-2.556178	0.074331	-0.000289
5	1	0	-1.443579	-1.412763	-0.000051
6	16	0	1.184187	0.032217	0.000054

CH_3CS

Centre Number	Atomic Number	Atomic Type	Coordinates (Angstroms) X	Y	Z
1	6	0	0.333950	-0.440286	-0.000074
2	6	0	1.698741	0.123674	-0.000035
3	1	0	2.236013	-0.247148	0.878851
4	1	0	2.238016	-0.250686	-0.876155
5	1	0	1.710879	1.220276	-0.002139
6	16	0	-1.148816	0.073577	0.000006

cis-HOPO

Centre Number	Atomic Number	Atomic Type	Coordinates (Angstroms) X	Y	Z
1	15	0	0.140377	-0.491164	0.000001
2	8	0	1.227129	0.527630	-0.000001
3	8	0	-1.327652	0.241376	-0.000002
4	1	0	-1.301470	1.215417	0.000013

TCProt

Centre Number	Atomic Number	Atomic Type	Coordinates (Angstroms) X	Y	Z
1	17	0	-3.138529	-0.875720	0.000055
2	17	0	2.197428	-1.819754	-0.000044
3	17	0	2.617113	1.360634	0.000093
4	8	0	-2.180384	1.993004	-0.000320
5	7	0	0.020924	1.515015	0.000060
6	6	0	-1.219732	1.059760	0.000150
7	6	0	-1.492632	-0.318943	0.000002
8	6	0	-0.437412	-1.212394	0.000011
9	6	0	0.865142	-0.721406	-0.000072
10	6	0	1.031008	0.667427	-0.000171
11	1	0	-3.054072	1.577902	0.000838
12	1	0	-0.619776	-2.281401	0.000018

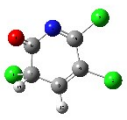

Centre Number	Atomic Number	Atomic Type	Coordinates (Angstroms) X	Y	Z
1	17	0	-2.439512	-0.799202	-1.155515
2	17	0	2.286071	-1.517999	0.398474
3	17	0	2.166827	1.445136	-0.715747
4	8	0	-2.210396	1.599485	1.321825
5	7	0	-0.277185	1.506291	0.113887
6	6	0	-1.436515	0.935855	0.687118
7	6	0	-1.663623	-0.555318	0.459041
8	6	0	-0.383450	-1.322088	0.518198
9	6	0	0.777618	-0.689258	0.321546
10	6	0	0.739370	0.760448	-0.023073
11	1	0	-2.386604	-0.899779	1.198196
12	1	0	-0.417890	-2.392862	0.690408

Centre Number	Atomic Number	Atomic Type	Coordinates (Angstroms) X	Y	Z
1	17	0	3.142983	0.794482	-0.220979
2	17	0	-2.187095	1.805379	0.111300
3	17	0	-2.598293	-1.374149	-0.180214
4	8	0	2.226012	-1.982488	0.348330
5	7	0	0.000390	-1.523968	-0.024997
6	6	0	1.324401	-1.183362	0.160144
7	6	0	1.564700	0.255715	-0.002862
8	6	0	0.483307	1.230687	0.100555
9	6	0	-0.884485	0.698704	0.050007
10	6	0	-1.011758	-0.673992	-0.023155
11	1	0	0.619561	1.610306	1.139697
12	1	0	0.633510	2.113758	-0.531316

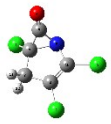

Centre Number	Atomic Number	Atomic Type	Coordinates (Angstroms) X	Y	Z
1	17	0	-2.797416	-0.737479	-0.845444
2	17	0	2.394600	-1.556787	0.346008
3	17	0	1.969497	1.645833	-0.720915
4	8	0	-1.560688	1.700141	1.761592
5	7	0	-0.611427	0.925836	-0.362334
6	6	0	-1.328839	0.994640	0.836694
7	6	0	-1.400995	-0.271413	0.103802
8	6	0	-0.410931	-1.383700	0.471436
9	6	0	0.911068	-0.722852	0.164732
10	6	0	0.763405	0.531986	-0.272350

11	1	0	-0.492118	-1.686515	1.520078
12	1	0	-0.578206	-2.264058	-0.156415

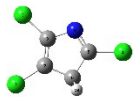

Centre Number	Atomic Number	Atomic Type	Coordinates (Angstroms) X	Y	Z
1	17	0	3.194532	-0.003313	0.000074
2	17	0	-2.140262	-1.597554	0.000077
3	17	0	-1.798891	1.833459	-0.000014
4	7	0	0.789250	1.077942	0.000004
5	6	0	1.476774	0.003454	-0.000092
6	6	0	0.678049	-1.270161	-0.000187
7	6	0	-0.699208	-0.680567	-0.000066
8	6	0	-0.562728	0.656354	0.000018
9	1	0	0.888212	-1.877060	-0.887935
10	1	0	0.888267	-1.877086	0.887535

2,3,5-TCPyridine

Centre Number	Atomic Number	Atomic Type	Coordinates (Angstroms) X	Y	Z
1	17	0	-3.414271	0.192384	0.000280
2	17	0	1.714010	1.930433	-0.000200
3	17	0	2.630908	-1.156511	0.000440
4	7	0	0.074787	-1.703241	-0.000558
5	6	0	-1.228376	-1.429371	-0.000502
6	6	0	-1.702143	-0.121383	0.000024
7	6	0	-0.795278	0.931935	0.000146
8	6	0	0.562382	0.634774	-0.000193
9	6	0	0.946775	-0.715077	-0.000176
10	1	0	-1.131113	1.960725	0.000204
11	1	0	-1.913550	-2.270500	-0.000937

TCP ipso H adduct

Centre Number	Atomic Number	Atomic Type	Coordinates (Angstroms) X	Y	Z
1	17	0	3.182374	-0.819318	0.154430
2	17	0	-2.091595	-1.882890	-0.191437
3	17	0	-2.705387	1.235869	0.118045
4	8	0	1.923805	1.833601	-0.806343
5	7	0	-0.127065	1.541738	0.273150
6	6	0	1.277742	1.169716	0.259065
7	6	0	1.535468	-0.306137	0.110322
8	6	0	0.519348	-1.204725	-0.020128
9	6	0	-0.811204	-0.748512	-0.016120
10	6	0	-1.043862	0.667281	0.134816

11	1	0	1.662340	2.761093	-0.749280
12	1	0	0.721818	-2.263421	-0.122483
13	1	0	1.698238	1.503367	1.225085

c-C_2H_4SO (b3lyp/6-31G(2df,p) optimisation)

Centre Number	Atomic Number	Atomic Type	Coordinates (Angstroms) X	Y	Z
1	6	0	-1.248600	-0.000122	-0.794741
2	6	0	-1.248536	-0.000840	0.794785
3	1	0	-1.561550	-0.919432	-1.278080
4	1	0	-1.561843	0.919898	-1.276549
5	1	0	-1.561574	0.918686	1.277669
6	1	0	-1.561618	-0.920641	1.277100
7	16	0	0.314563	0.000009	-0.000035
8	8	0	1.011457	1.266868	0.000237
9	8	0	1.013092	-1.265978	-0.000216

c-$C_2H_4SO_2$ (b3lyp/6-31G(2df,p) optimisation)

Centre Number	Atomic Number	Atomic Type	Coordinates (Angstroms) X	Y	Z
1	6	0	-1.248600	-0.000122	-0.794741
2	6	0	-1.248536	-0.000840	0.794785
3	1	0	-1.561550	-0.919432	-1.278080
4	1	0	-1.561843	0.919898	-1.276549
5	1	0	-1.561574	0.918686	1.277669
6	1	0	-1.561618	-0.920641	1.277100
7	16	0	0.314563	0.000009	-0.000035
8	8	0	1.011457	1.266868	0.000237
9	8	0	1.013092	-1.265978	-0.000216

SO_2 (b3lyp/6-31G(2df,p) optimisation)

Centre Number	Atomic Number	Atomic Type	Coordinates (Angstroms) X	Y	Z
1	16	0	0.000000	0.364953	0.000000
2	8	0	1.244426	-0.364966	0.000000
3	8	0	-1.244426	-0.364940	0.000000

O_2 (b3lyp/6-31G(2df,p) optimisation)

Centre Number	Atomic Number	Atomic Type	Coordinates (Angstroms) X	Y	Z
1	8	0	0.000000	0.000000	0.603218
2	8	0	0.000000	0.000000	-0.603218

HOP(OO)OS (^{3}A) b3lyp/6-31G(2df,p) optimisation

Centre Number	Atomic Number	Atomic Type	Coordinates (Angstroms) X	Y	Z
1	16	0	-1.622364	0.039902	-0.799380
2	15	0	0.207016	-0.127903	0.096385
3	8	0	1.106815	-1.261401	-0.105849
4	8	0	0.897469	1.305017	0.030379
5	1	0	1.859144	1.238274	0.116893
6	8	0	-1.681881	0.122511	1.679068
7	8	0	-0.390074	-0.098532	1.747620

$HOPO_2$ b3lyp/6-31G(2df,p) optimisation

Centre Number	Atomic Number	Atomic Type	Coordinates (Angstroms) X	Y	Z
1	15	0	0.086556	0.105554	0.000105
2	8	0	-0.744648	1.304764	-0.000052
3	8	0	-0.738716	-1.247043	-0.000001
4	1	0	-1.691270	-1.077153	0.000056
5	8	0	1.520941	-0.130793	-0.000077

SO ($^3\Sigma_g$) b3lyp/6-31G(2df,p) optimisation

Centre Number	Atomic Number	Atomic Type	Coordinates (Angstroms) X	Y	Z
1	16	0	0.193797	0.450450	0.000000
2	8	0	-1.303037	0.450450	0.000000

TS for C_2H_4 + HOPOS → c-C_2H_4S + cis-HOPO

Centre Number	Atomic Number	Atomic Type	Coordinates (Angstroms) X	Y	Z
1	6	0	-2.818419	0.653030	0.322519
2	6	0	-2.762859	-0.717909	0.307247
3	1	0	-3.224285	1.207171	-0.516266
4	1	0	-2.576743	1.213823	1.218119
5	1	0	-2.479534	-1.276595	1.191794
6	1	0	-3.125408	-1.284423	-0.543084
7	16	0	-0.769823	0.053209	-0.455586
8	15	0	1.420942	0.134425	-0.249837
9	8	0	2.194372	1.196172	0.431704
10	8	0	1.956381	-1.330174	0.202430
11	1	0	2.690642	-1.266413	0.834700

TS for c-$C_2H_4S \rightarrow CH_3SCH$

Centre Number	Atomic Number	Atomic Type	Coordinates (Angstroms) X	Y	Z
1	6	0	0.245399	-1.430319	-0.163910
2	6	0	0.921499	0.604844	0.252168
3	1	0	0.850239	-1.291874	-1.086554
4	1	0	1.524685	-0.253940	0.628456
5	1	0	0.835547	1.265547	1.113980
6	1	0	1.411089	1.067203	-0.601881
7	16	0	-0.779535	0.038402	-0.142296

TS for ^{3}•CH_2CH_2S• $\rightarrow CH_3CHS$

Centre Number	Atomic Number	Atomic Type	Coordinates (Angstroms) X	Y	Z
1	6	0	1.594999	-0.337115	-0.015972
2	6	0	0.423842	0.610611	0.066785
3	1	0	1.429273	-1.380190	0.222727
4	1	0	2.466923	-0.045529	-0.588705
5	1	0	1.251268	0.372009	1.018748
6	1	0	0.594656	1.593846	-0.359314
7	16	0	-1.136585	-0.141332	-0.055491

TS for ^{3}•CH_2CH_2S• $\rightarrow CH_2CHSH$

Centre Number	Atomic Number	Atomic Type	Coordinates (Angstroms) X	Y	Z
1	6	0	1.699375	-0.420016	-0.065975
2	6	0	0.671274	0.587512	-0.241980
3	1	0	2.213781	-0.549022	0.880238
4	1	0	1.846090	-1.180708	-0.828173
5	1	0	-0.136652	0.970015	0.943550
6	1	0	0.827323	1.489605	-0.827312
7	16	0	-1.056963	0.200426	0.139821

TS for HCS + HOPOS $\rightarrow$ HCSS + HOPO (b3lyp/6-31G(2df,p) optimisation)

Centre Number	Atomic Number	Atomic Type	Coordinates (Angstroms) X	Y	Z
1	6	0	2.043535	-0.447719	0.293167
2	1	0	1.758625	-1.318960	0.879042
3	16	0	3.420953	0.221896	-0.030074
4	16	0	-0.043140	0.453805	-0.585918
5	15	0	-1.899563	-0.083497	-0.353827
6	8	0	-2.699316	-1.176764	-0.931901
7	8	0	-2.519492	0.481006	1.015341
8	1	0	-3.376058	0.064107	1.190640

TS for c-$C_2H_3S \rightarrow CH_2CHS$

Centre Number	Atomic Number	Atomic Type	Coordinates (Angstroms) X	Y	Z
1	6	0	-0.558252	0.786932	-0.095890
2	6	0	-1.205513	-0.439417	0.039683
3	1	0	-0.745078	1.710999	0.436994
4	1	0	-1.791730	-0.699839	0.925166
5	1	0	-1.246754	-1.143742	-0.782990
6	16	0	0.916434	-0.090701	-0.133387

TS for $CH_2CHS \rightarrow CH_3CS$

Centre Number	Atomic Number	Atomic Type	Coordinates (Angstroms) X	Y	Z
1	6	0	0.331126	0.324252	-0.040593
2	6	0	1.595143	-0.181150	0.203143
3	1	0	1.143666	0.404930	-0.989562
4	1	0	2.443840	0.495982	0.258119
5	1	0	1.780469	-1.238554	0.417413
6	16	0	-1.227777	-0.089168	-0.136900

TS for $HCSS \rightarrow H + CS_2$

Centre Number	Atomic Number	Atomic Type	Coordinates (Angstroms) X	Y	Z
1	6	0	-0.000661	0.114426	0.000000
2	1	0	0.002185	1.957756	0.000000
3	16	0	-1.570212	-0.086577	0.000000
4	16	0	1.568300	-0.091428	0.000000

TS for TCP + H → TCP ipso H adduct (b3lyp/6-31G(2df,p) optimisation)

Centre Number	Atomic Number	Atomic Type	Coordinates (Angstroms) X	Y	Z
1	17	0	3.138870	-0.903877	-0.050159
2	17	0	-2.191535	-1.845951	0.012949
3	17	0	-2.640888	1.344453	-0.049273
4	8	0	2.219861	1.930577	-0.101065
5	7	0	-0.039852	1.506269	-0.002366
6	6	0	1.224004	1.049007	0.100222
7	6	0	1.504549	-0.345049	-0.004137
8	6	0	0.443376	-1.226174	-0.014492
9	6	0	-0.864161	-0.734001	0.014004
10	6	0	-1.042602	0.657988	0.002663
11	1	0	1.817059	2.809755	-0.097027
12	1	0	0.619572	-2.293447	-0.050789
13	1	0	1.282850	0.975937	1.853563

TS for TCP ipso H adduct → 2,3,5-TCPyridine (b3lyp/6-31G(2df,p) optimisation)

Centre Number	Atomic Number	Atomic Type	Coordinates (Angstroms) X	Y	Z
1	17	0	3.210822	0.704503	-0.287751
2	17	0	-2.020320	1.891154	0.344064
3	17	0	-2.679912	-1.191419	-0.262339
4	8	0	1.665083	-1.749001	1.453000
5	7	0	-0.099485	-1.489602	-0.504579
6	6	0	1.197355	-1.113177	-0.455023
7	6	0	1.548009	0.239805	-0.246835
8	6	0	0.558709	1.170861	0.013469
9	6	0	-0.766864	0.745662	0.024683
10	6	0	-1.036804	-0.613798	-0.242918
11	1	0	0.964466	-2.422630	1.485318
12	1	0	0.801785	2.208779	0.199389
13	1	0	1.927029	-1.815117	-0.834472

TS for c-C_2H_4S + O_2 → c-C_2H_4SO + O (b3lyp/6-31G(2df,p) optimisation)

Centre Number	Atomic Number	Atomic Type	Coordinates (Angstroms) X	Y	Z
1	6	0	-0.997157	-0.236495	-0.731710
2	6	0	-1.266186	0.116611	0.680392
3	1	0	-1.724919	-0.819175	-1.284147
4	1	0	-0.332356	0.423942	-1.286661
5	1	0	-0.807324	1.021816	1.064922
6	1	0	-2.193109	-0.193950	1.150753
7	16	0	-0.010638	-1.206380	0.483510
8	8	0	1.440035	-0.224222	0.362043
9	8	0	1.728889	1.045909	-0.597776

TS for c-C_2H_4SO + O → C_2H_4 + SO_2 (b3lyp/6-31G(2df,p) optimisation)

Centre Number	Atomic Number	Atomic Type	Coordinates (Angstroms) X	Y	Z
1	6	0	-0.492991	1.048217	-0.772020
2	6	0	-0.366815	1.206547	0.696088
3	1	0	-1.468983	0.909757	-1.215123
4	1	0	0.271112	1.500288	-1.395706
5	1	0	0.449793	1.807876	1.081031
6	1	0	-1.254711	1.130408	1.309458
7	16	0	0.290106	-0.437081	0.088294
8	8	0	1.769514	-0.308825	-0.096266
9	8	0	-1.454522	-1.176627	0.004170

TS for c-$C_2H_4SO + O_2 \rightarrow$ c-$C_2H_4SO_2$ + O (b3lyp/6-31G(2df,p) optimisation)

Centre Number	Atomic Number	Atomic Type	Coordinates (Angstroms) X	Y	Z
1	6	0	-0.330117	1.223514	-0.711915
2	6	0	-0.479976	1.306850	0.820211
3	1	0	-1.192085	1.505329	-1.306842
4	1	0	0.652438	1.428373	-1.124301
5	1	0	0.396630	1.561909	1.405011
6	1	0	-1.438136	1.623425	1.218195
7	16	0	-0.467774	-0.347738	0.105593
8	8	0	1.156600	-0.835868	0.134249
9	8	0	-1.770301	-1.018101	-0.071515
10	8	0	2.421245	-0.077901	-0.468622

TS for c-$C_2H_4SO_2 \rightarrow C_2H_4 + SO_2$ (b3lyp/6-31G(2df,p) optimisation)

Centre Number	Atomic Number	Atomic Type	Coordinates (Angstroms) X	Y	Z
1	6	0	-1.471732	0.000120	-0.760847
2	6	0	-1.387751	0.000001	0.677215
3	1	0	-1.600280	-0.933379	-1.289727
4	1	0	-1.600245	0.933713	-1.289575
5	1	0	-1.574653	0.912947	1.237694
6	1	0	-1.574781	-0.913020	1.237536
7	16	0	0.439336	-0.000012	0.204639
8	8	0	1.029952	1.286557	-0.166740
9	8	0	1.029734	-1.286657	-0.166806

TS for HOPOS + $O_2 \rightarrow$ HOP(OO)OS (^{3}A) (b3lyp/6-31G(2df,p) optimisation)

Centre Number	Atomic Number	Atomic Type	Coordinates (Angstroms) X	Y	Z
1	16	0	-1.622364	0.039902	-0.799380
2	15	0	0.207016	-0.127903	0.096385
3	8	0	1.106815	-1.261401	-0.105849
4	8	0	0.897469	1.305017	0.030379
5	1	0	1.859144	1.238274	0.116893
6	8	0	-1.681881	0.122511	1.679068
7	8	0	-0.390074	-0.098532	1.747620

TS for HOP(OO)OS (^{3}A) → $HOPO_2$ + SO ($^3\Sigma_g$) (b3lyp/6-31G(2df,p) optimisation)

Centre Number	Atomic Number	Atomic Type	Coordinates (Angstroms) X	Y	Z
1	16	0	1.268615	-0.963047	0.018847
2	15	0	-0.641295	0.052454	-0.120478
3	8	0	-1.513707	-0.288913	-1.241881
4	8	0	-1.301911	-0.072759	1.321770
5	1	0	-2.149796	-0.535087	1.282984
6	8	0	1.545928	0.901535	0.030565
7	8	0	0.102262	1.484687	-0.080776

S5. Mechanism of formation of sulfur dioxide in oxidative decomposition.

One model we have derived for formation of SO_2 in oxidative decomposition of chlorpyrifos involves the initial reaction between thiirane and molecular O_2 ($^3\Sigma_g$) to form thiirane, 1-oxide and O (^{3}P). This is reaction R12

$$c\text{-}C_2H_4S + O_2 \rightarrow c\text{-}C_2H_4S{=}O + O \qquad (R12)$$

which takes place on the triplet PES. We have located a TS for this reaction which has a barrier, $\Delta H^{\ddagger}_{298}$ = 274 kJ mol^{-1}. This reaction is followed by the reaction between O atom and thiirane, 1-oxide.

$$O + c\text{-}C_2H_4S{=}O \rightarrow C_2H_4 + SO_2 \qquad (R13)$$

As one of the reactants, O (^{3}P), is a triplet, but both of the products, C_2H_4 and SO_2, are singlets, the reaction starts out of the triplet PES but at a certain stage in the reaction, must cross to the singlet surface. To determine if the intersystem crossing might be rate-determining, we have investigated the potential energy surface of the approaching O atom to the S atom. In Figure S4 we show the variation in the triplet and singlet energies as a function of decreasing S-O distance. The singlet energies were all calculated after removal of any triplet contamination in the wavefunction using the option stable=opt in Gaussian 09. The ordinate is the electronic energy relative to that of separated c-C_2H_4SO + O (^{3}P). Starting at the right of the Figure, we see that as the S-O distance decreases, the energy rises to a maximum at r_{SO} =1.897 Å, corresponding to the TS (labelled), *still on the triplet surface*. The barrier with respect to the reactants, calculated at G4MP2, is only 2.4 kJ mol^{-1} at 0 K. Since at the barrier the TS is a pure triplet, it can be described by a single reference treatment and the rate parameters of the reaction can be expressed in terms of the partition functions of TS and reactants. Intersystem crossing takes place at a S-O distance shorter by approximately 0.03 Å.

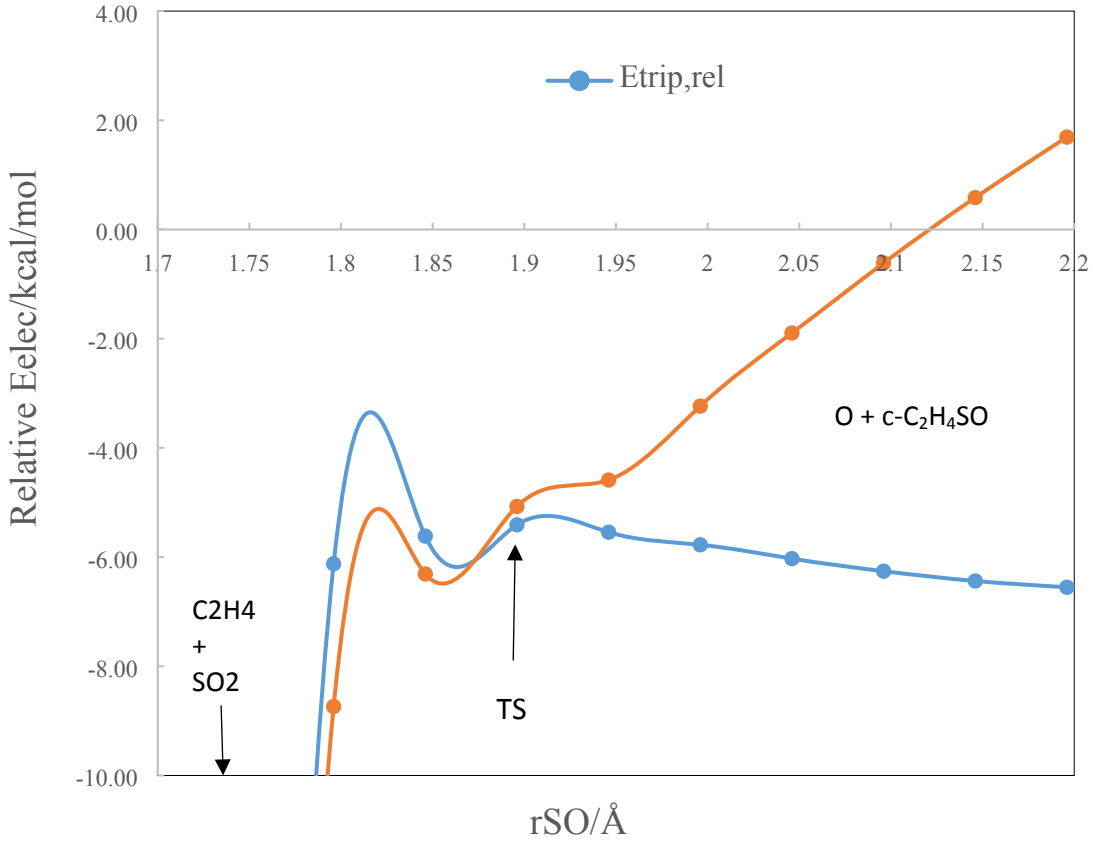

Figure S4: Variation of the electronic energies of triplet (blue) and singlet (orange) with distance r_{SO} between approaching O atom and the S atom of thiirane, 1-oxide. Calculated at B3LYP/6-31G(2df,p).

The reaction is extremely exothermic with an enthalpy of reaction of -468 kJ mol^{-1} at 298 K. The reaction is also very fast. Using ChemRate[S1] to evaluate the rate constant, we obtain the value of $k_{R13} = 3.03\times10^{12}$ exp(-11.8 kJ mol^{-1}/RT) cm^3 mol^{-1} s^{-1}.

On account of the high barrier for reaction R12, the above model for SO_2 formation is likely to be important only at quite high temperatures (>~1300 K). We have also been able to develop a mechanism of formation of SO_2 from HOPOS and O_2 which does not have a high barrier for initiation. Reaction between HOPOS and O_2 ($^3\Sigma_g$) commences on the triplet surface and culminates with the formation of the adduct HOP(OO)OS (^{3}A) whose structure is shown in Figure S5.

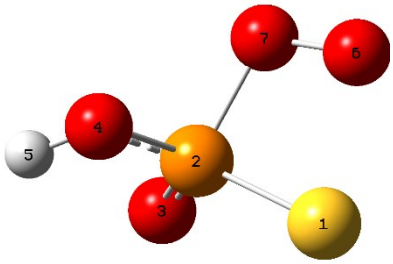

Figure S5: Structure of adduct HOP(OO)OS (^{3}A) optimised at the b3lyp/6-31G(2df,p) level of theory

Single configuration DFT methods do not lead to a stable singlet adduct comparable with this triplet. It is important to determine where a possible singlet adduct is located relative to the energy of the triplet and to ascertain whether the reaction continues on the triplet surface.

We therefore used the multiconfiguration CASSCF(6,6) method (6 electrons in 6 orbitals) to investigate the triplet-singlet splitting in the adduct. Three different basis sets have been employed, viz., 6-31G(d,p), cc-PVDZ and cc-PVTZ. All basis sets produced an optimised singlet adduct whose structure closely resembled that of the CASSCF optimised triplet, most bondlengths differed by just a few hundreths of an Ångstom and bond angles by a few tenths of a degree. All basis sets found the singlet at the triplet geometry to lie at a higher energy. The resultant energies were, respectively, 4.7 kJ mol^{-1}, 230 J mol^{-1} and 130 J mol^{-1}. Hence formation of the triplet adduct takes place on the triplet surface and further reaction will therefore take place also on the triplet surface.

As the peripheral oxygen atom, O_6, approaches the sulfur atom as, for example, in bending of the $O_6O_7P_2$ angle, fission of the nascent SO bond takes place. We have located a TS for this fission and the screen shot from Gaussian09 in Figure S6 clearly shows progress of this reaction from triplet HOP(OO)OS to $HOPO_2$ + SO ($^3\Sigma_g$) through the TS.

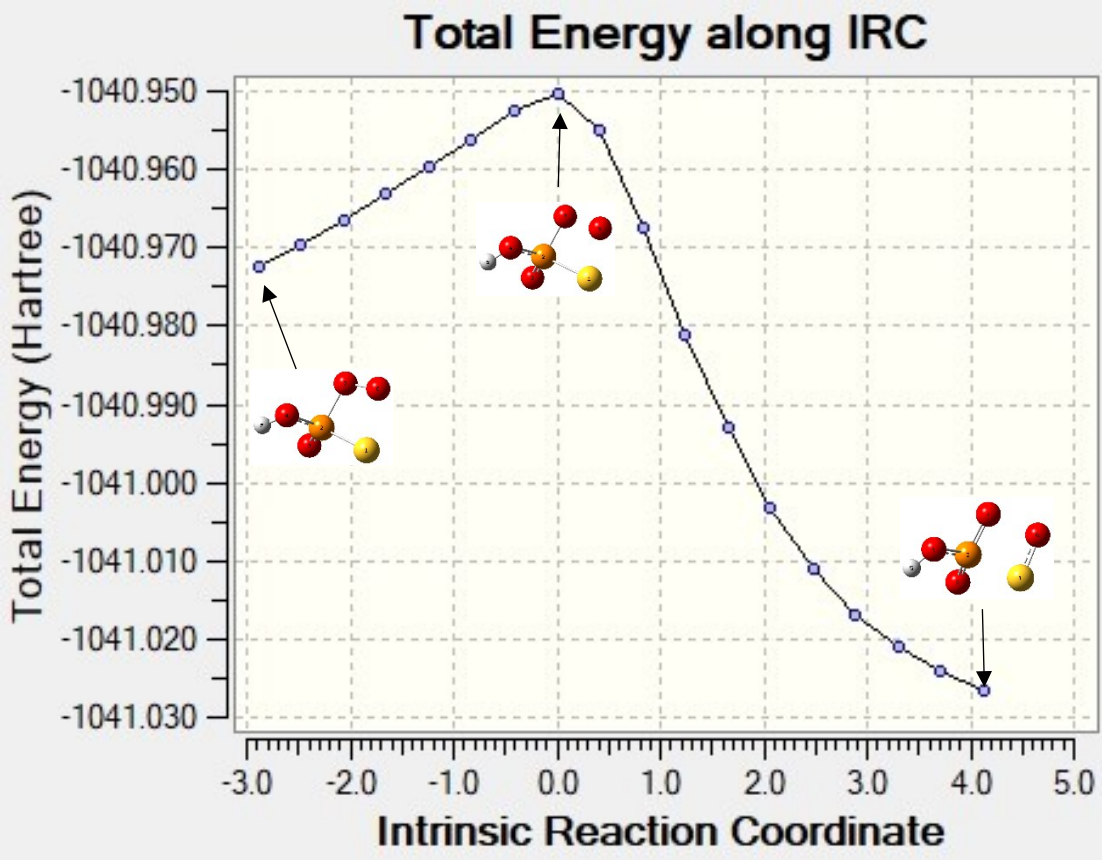

Figure S6: Intrinsic reaction coordinate diagram for reaction of HOP(OO)OS (^{3}A) → $HOPO_2$ + SO ($^3\Sigma_g$). Reactant, TS and products are indicated.

The final reaction (R16 in the MS) has been well-studied. Most studies, however, range from about 200 – 500 K. We have chosen the rate constant of Garland[S2] as it was studied over the range of 250 – 3500 K and is in good agreement with the several low temperature studies.

References

(S1) V. Mokrushin, V. Bedanov, W. Tsang, M. Zachariah, V. Knyazev and W. S. McGivern, ChemRate, version 1.5.10, *NIST: Gaithersburg, MD*, 2011.

(S2) N. L. Garland, Temperature dependence of the reaction: SO+O2, *Chemical Physics Letters*, 1998, **290**, 385-39